Evidence for Precipitation on Mars from Dendritic Valleys in the Valles Marineris Area

Nicolas Mangold *et al.*

Science **305**, 78 (2004);
DOI: 10.1126/science.1097549

Science (print ISSN 0036-8075; online ISSN 1095-9203) is published weekly, except the last week in December, by the American Association for the Advancement of Science, 1200 New York Avenue NW, Washington, DC 20005.

4. B. Asfaw *et al.*, *Nature* **416**, 317 (2002).
5. E. Abbate *et al.*, *Nature* **393**, 458 (1998).
6. G. C. Conroy, C. J. Jolly, D. Cramer, J. E. Kalb, *Nature* **276**, 67 (1978).
7. G. P. Rightmire, *Am. J. Phys. Anthropol.* **61**, 245 (1983).
8. G. P. Rightmire, *J. Hum. Evol.* **31**, 21 (1996).
9. J. J. Hublin, in *Human Roots: Africa and Asia in the Middle Pleistocene*, L. Barham, K. Robson-Brown, Eds. (Western Academic & Specialist Press, Bristol, UK, 2001), pp. 99–121.
10. J.-L. Arsuaga *et al.*, *J. Hum. Evol.* **37**, 431 (1999).
11. G. Manzi, F. Mallegni, A. Ascenzi, *Proc. Natl. Acad. Sci. U.S.A.* **98**, 10011 (2001).
12. G. Manzi, E. Bruner, P. Passarello, *J. Hum. Evol.* **44**, 731 (2003).
13. W. H. Gilbert, T. D. White, B. Asfaw, *J. Hum. Evol.* **45**, 255 (2003).
14. G. P. Rightmire, *Evol. Anthropol.* **6**, 218 (1998).
15. I. Tattersall, *J. Hum. Evol.* **15**, 165 (1986).
16. M. H. Wolpoff, A. G. Thorne, J. Jelínek, Y. Zhang, *Cour. Forschungsinst. Senckenb.* **171**, 341 (1994).
17. G. Ll. Isaac, *Olorgesailie: Archaeological Studies of a Middle Pleistocene Lake Basin in Kenya* (Univ. of Chicago Press, Chicago, IL, 1977).
18. R. Potts, A. K. Behrensmeyer, P. Ditchfield, *J. Hum. Evol.* **37**, 747 (1999).
19. A. Deino, R. Potts, *J. Geophys. Res.* **95,** 8453 (1990).
20. L. Tauxe, A. L. Deino, A. K. Behrensmeyer, R. Potts, *Earth Planet. Sci. Lett.* **109**, 561 (1992).
21. Y. Hou *et al.*, *Science* **287**, 1622 (2000).
22. A. M. Sarna-Wojcicki, M. S. Pringle, J. Wijbrans, *J. Geophys. Res.* **105**, 21431 (2000).
23. S. C. Antón, *Am. J. Phys. Anthropol.* **102**, 497 (1997).
24. L. Gabunia *et al.*, *Science* **288**, 1019 (2000).
25. S. C. Antón, *J. Hum. Evol.* **46**, 335 (2004).
26. F. Mallegni *et al.*, *C. R. Paleovol.* **2**, 153 (2003).
27. Olorgesailie research is conducted in collaboration with the National Museums of Kenya (NMK), with excavation licenses granted by the Kenyan government. This work was funded by NSF (grant BCS-0218511) and the Smithsonian Institution's Human Origins Program. We thank I. O. Farah, M. G. Leakey, E. Mbua, M. Muungu, S. N. Muteti, and the staff of the NMK Palaeontology Division for support. The analysis and manuscript benefited from discussions with S. Antón, F. Spoor, and B. Wood.

Supporting Online Material

www.sciencemag.org/cgi/content/full/305/5680/75/DC1
SOM Text
Tables S1 and S2
References

8 March 2004; accepted 25 May 2004

Evidence for Precipitation on Mars from Dendritic Valleys in the Valles Marineris Area

Nicolas Mangold,[1*] Cathy Quantin,[2] Véronique Ansan,[1] Christophe Delacourt,[2] Pascal Allemand[2]

Dendritic valleys on the plateau and canyons of the Valles Marineris region were identified from Thermal Emission Imaging System (THEMIS) images taken by Mars Odyssey. The geomorphic characteristics of these valleys, especially their high degree of branching, favor formation by atmospheric precipitation. The presence of inner channels and the maturity of the branched networks indicate sustained fluid flows over geologically long periods of time. These fluvial landforms occur within the Late Hesperian units (about 2.9 to 3.4 billion years old), when Mars was thought to have been cold. Our results suggest a period of warmer conditions conducive to hydrological activity.

The formation of valley networks on Mars has been the subject of considerable scientific debate (*1–4*). Valleys were attributed to fluvial erosion implying a warm and wet climate on early Mars (*5*), possibly conducive to biological activity (*6*). Several recent observations argue in favor of such conditions on early Mars (*7*, *8*), but valley networks could also have formed by water-lubricated debris flows (*4*), hydrothermal activity (*9*, *10*), or groundwater sapping (*11–13*) due to geothermal activity (*14*), and these hypotheses do not require conditions warmer than the current cold climate.

Here, we describe terrestrial-like dendritic valleys identified using THEMIS images (*15*) of the Mars Odyssey mission. These valleys are located in the Valles Marineris region (Fig. 1) on the plateau west of Echus Chasma (Fig. 2) and on the inner plateau west of Melas Chasma (Fig. 3). These landforms occur within Late Hesperian units (*16*), about 2.9 to 3.4 billion years old (*17*); they are thus unexpectedly younger than the Noachian (*16*) period, which is considered to be the potential primitive warm period (*4*).

The plateau west of Echus Chasma (0°N, 81°W) is covered by densely branched valleys that are frequently sinuous and extend over tens of kilometers (Fig. 2). Infrared (IR) images taken at night by THEMIS (Fig. 2A) show mainly intrinsic thermal properties of the ground (*15*). Valleys buried under loose material are outlined by variations of the thermal signal and resemble terrestrial deserts where sand covers the floor of dry valleys (fig. S1). On drainage basin G, the main valley is larger upstream than downstream close to the mouth, implying a thicker mantling at this location. With the exception of this place, most valleys have widths increasing from their sources to their mouth, as seen in terrestrial valleys. An IR image taken during the day by THEMIS shows that these dendritic valleys have their heads scattered at random points on the plateau (Fig. 2C). Hills

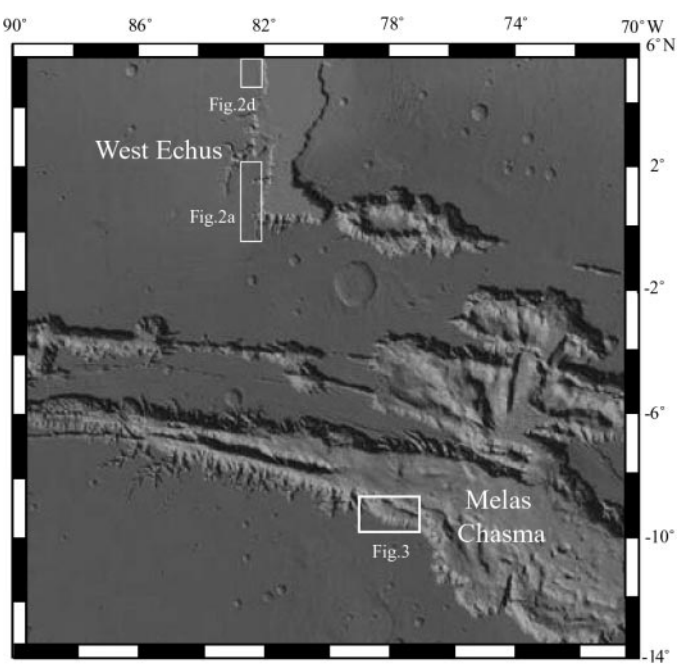

Fig. 1. MOLA shaded relief map of West Valles Marineris and the neighboring canyons. White squares indicate valley networks observed over Hesperian geologic units on THEMIS images of Figs. 2 and 3.

[1]Laboratoire IDES, UMR CNRS and Université Paris-Sud, Orsay Campus, 91405 Orsay, France. [2]Laboratoire des Sciences de la Terre, UMR CNRS UCB Lyon 1 and ENS Lyon, La Doua Campus, 69622 Villeurbanne, France.

*To whom correspondence should be addressed. E-mail: mangold@geol.u-psud.fr

are also gullied by small valleys with heads at the crestline of the hill (Fig. 2D). These characteristics are similar to terrestrial features of surface runoff due to atmospheric precipitation.

These characteristics are inconsistent with subsurface seepage induced by hydrothermal activity because water would not seep at the crest of hills. Moreover, no valleys with theater-shaped heads are observed, as would be the case if sapping had occurred (*11*, *12*). Sapping has been invoked to explain the development of tributary canyons in the Valles Marineris region (*18*), such as the narrow tributaries of Echus Chasma, 1 to 3 km deep, that dissect the plateau borders. The main valleys of basins E, G, and I connect to the heads of tributaries, implying that these valleys were active during the formation of tributaries, as observed on Earth (fig. S1B). This contemporaneous activity suggests that the backward recession of tributary canyons by sapping was connected to the hydrological processes existing over the plateau.

Two drainage basins with dendritic valleys are also observed on THEMIS images (Fig. 3) of the inner plateau of west Melas Chasma (77.5°W, 10°S). Several valley heads located at the foot of the southern wall slopes would suggest subsurface seepage. However, most valley heads are located on the opposite perched interior plateau and along the divide separating both drainage basins, thus suggesting another source of water than seepage from canyon walls (*19*). THEMIS visible-light images also show the presence of meandering valleys (Fig. 3C) and inner channels (Fig. 3D) on the floor of some of these valleys, indicating surface conditions with stable liquid water and sustained fluvial activity (*20*, *21*).

The drainage densities (i.e., the total length of valleys divided by the area of each basin) vary from 0.6 to 1.0 km^{-1} for the nine basins of Echus Plateau measured using IR images at 100 m/pixel (table S1). The drainage densities in Melas Chasma are 1.1 km^{-1} and 1.5 km^{-1}, as measured using visible-light images at 18 m/pixel. By comparison, drainage densities of terrestrial valley networks are usually from 2 to 100 km^{-1}. However, such high densities are obtained with maximum-resolution mapping, whereas the same terrestrial networks mapped at the scale of Viking image mosaics (*22*) have densities of only 0.1 to 0.2 km^{-1}. Thus, densities measured at THEMIS resolution, a scale slightly better than Viking mosaics, are equivalent to terrestrial fluvial valleys mapped at the same scale. Additionally, morphometric parameters such as valley order, bifurcation ratio, and valley length ratio (*23*, *24*) give values similar to terrestrial river networks for the drainages of both regions (table S1 and fig. S2).

Precise depths of valleys are not measurable at the resolution of the Mars Observer Laser Altimeter (MOLA), but they can be estimated roughly from THEMIS images to a few tens of meters for widths of several hundreds of meters. These valleys, like rivers, are always oriented in the direction of the local slope (fig. S3). Moreover, the variations in the geometry of valleys are consistent with the variations of the slope, with dendritic valleys on nearly flat areas and subparallel valleys on slopes $>1.3°$ (fig. S3). This relationship is observed in experimental streams and terrestrial rivers formed by surface runoff due to precipitation by rainfall or snowmelt subsequent to snow deposition (*25*).

Snowmelt under a cold climate was proposed to explain some valley networks (*26*, *27*). However, alluvial valleys with inner channels (Fig. 3D) require stable liquid water, favoring subaerial flows under a warmer climate. Moreover, snow accumulation would create glaciers (*27*), but subglacial valleys are discontinuous with large undissected areas and abrupt inception and termination of valleys [e.g., (*28*)], unlike such dendritic valleys. The maturity of the valley networks is also inconsistent with short episodes of glacial outburst with large and braided channels. For example, terrestrial networks become mature (i.e., with fully branching patterns) only after several tens of

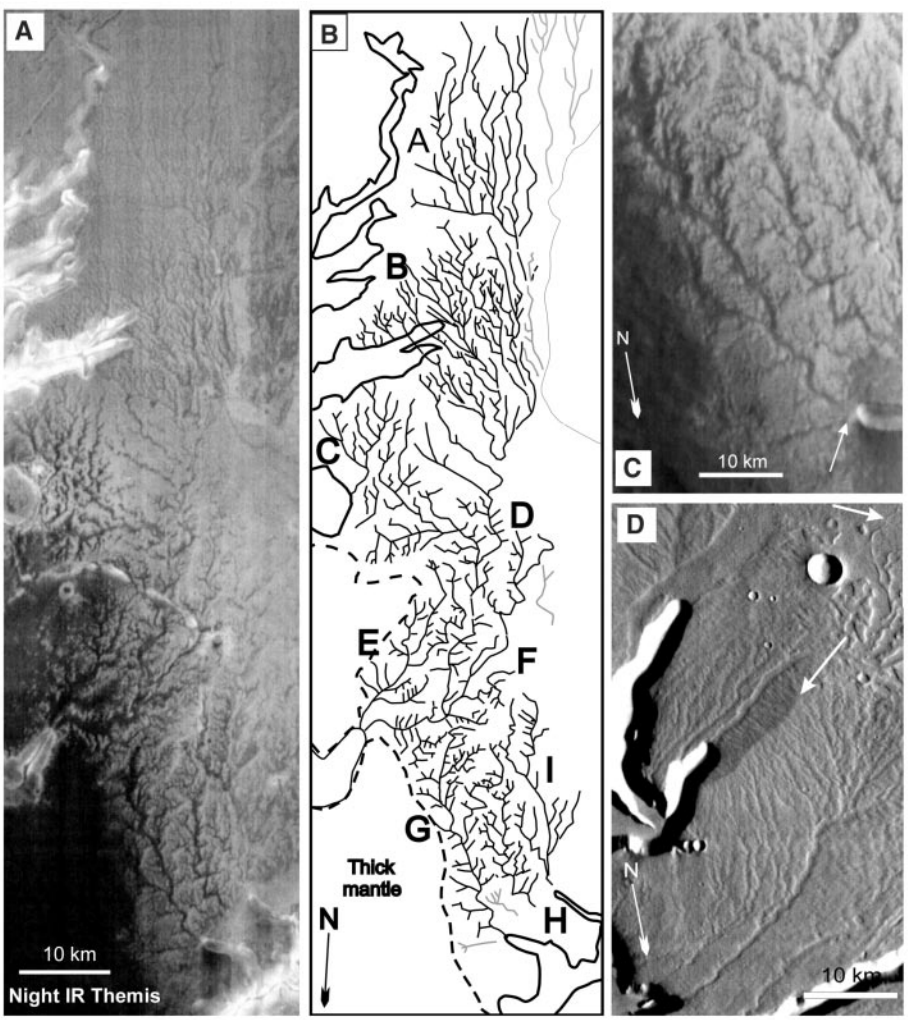

Fig. 2. Dense valley networks of West Echus Chasma plateau (0°N, 81°W). (**A**) Night IR THEMIS images (I02119003 and I0857003). At the lower left of the image, a dark area is due to the low temperature of loose material (sand or dust), whereas the right part of the image is rocky with a higher temperature. The plateau is located at the transition between regions of low and high thermal inertia, which makes the identification of valleys easier from differential mantling. Valleys at top left are dissected by deep canyon tributary of Echus Chasma. (**B**) Geomorphic map of West Echus Chasma. The observed networks can be separated into nine drainage basins from A to I. (**C**) Close-up over G, H, and I drainage basins on day IR THEMIS image (I06419047). Contrasts in brightness correspond to differences in albedo and/or topography. The arrow displays the junction of the main valley over the plateau with the head of the tributary canyon. (**D**) THEMIS day IR (I01950002). The central arrow indicates a linear hill covered by gullies that organize downstream in branching valleys on the illuminated flank. The top arrow indicates a zone of erosion of the upper layers with apparent preservation of an inverted channel (*29*).

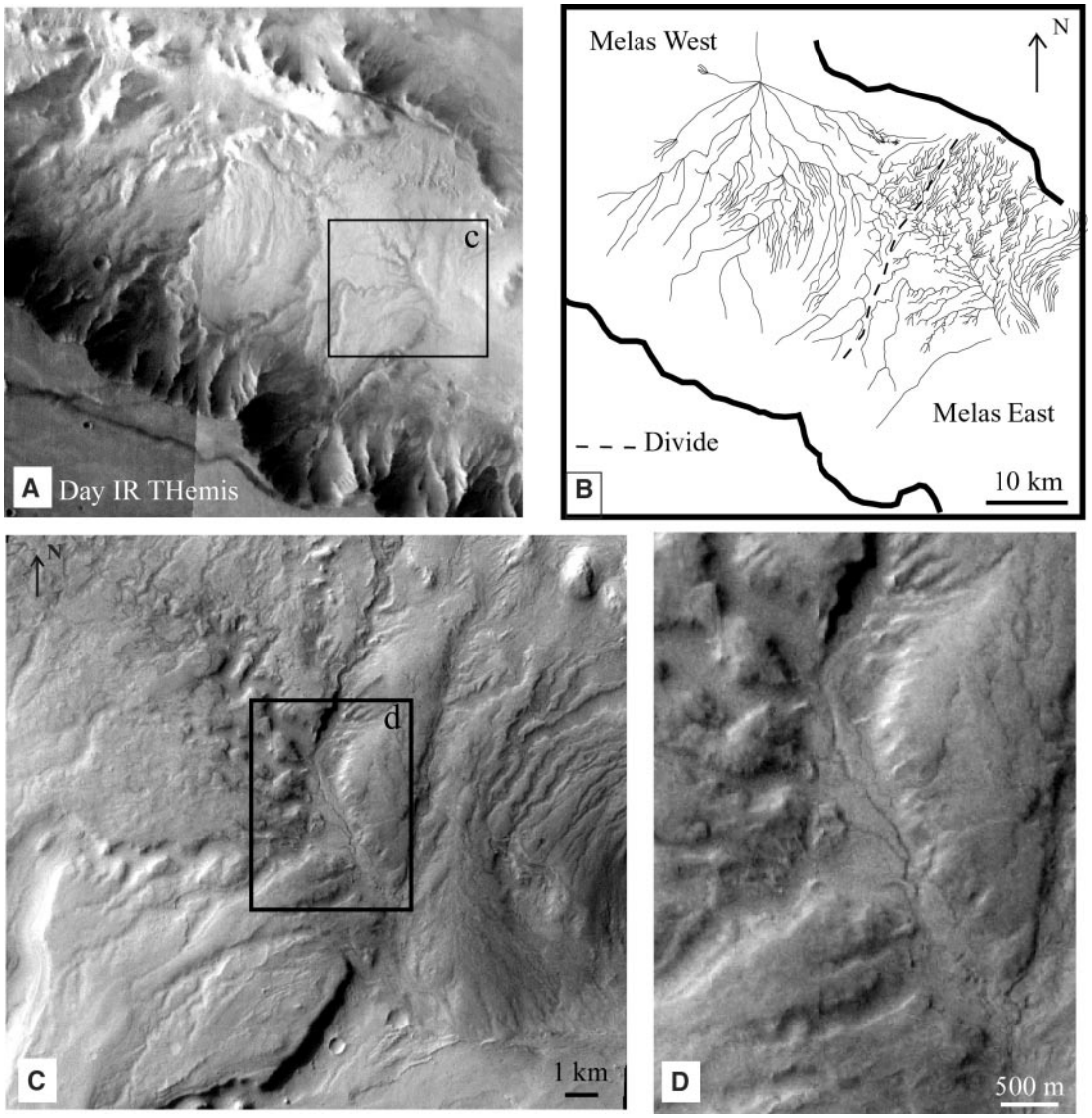

Fig. 3. Dense valley networks on West Melas Chasma inner plateau (77.5°W, 10°S). (**A**) Day IR THEMIS images (I06631017 and I06227001). (**B**) Valley network map drawn from a combination of IR and visible-light THEMIS images. Valleys are located on a perched surface around 2 km above the floor of Melas Chasma. They are separated by a divide in two drainage basins (West and East). (**C**) THEMIS visible-light image (V3249001) shows meandering valleys over East Melas drainage basin. (**D**) Close-up over the central valley with inner channels.

thousands of years of activity (*24*). The formation of dendritic valleys thus likely involves a relatively warm climate with liquid water stable at the surface.

If atmospheric processes are invoked, similar valleys should be observed elsewhere than in the Echus and Melas areas. Nonetheless, dust deposition could completely fill in valleys that are only a few tens of meters deep. Other valleys may be hidden beneath this mantle. No valleys exist west of the Echus plateau valleys except for some relics present in inverted topography (*29*) (Fig. 2D), demonstrating the role of wind erosion in the removal of the uppermost deposits. Differences in the strength of eroded rocks may play a role in the development or preservation of fluvial landforms. Mesoscale variations of the climate could also affect their distribution.

Echus Chasma plateau valleys formed over a Late Hesperian volcanic unit (*30*), and they are buried at the north by Early Amazonian lava flows, thus restricting their formation to that interval of time. The connections of the main valleys and the heads of tributary canyons (Fig. 2C) also imply an age contemporaneous with or slightly younger than the Echus canyon, which formed during the Late Hesperian. Melas Chasma valleys are younger than the development of Valles Marineris, as they developed on inner plateaus dated to the Late Hesperian epoch (*18*). Thus, they may have formed at the same period as Echus Chasma plateau valleys. The transition from a possible warm early Mars to a colder climate is usually dated to the Late Noachian–Early Hesperian boundary (*4*), about 3.6 billion years ago (*17*). The apparent age of the valleys suggests that significant fluvial activity occurred until the Late Hesperian.

Surface runoff in the Late Hesperian epoch could correspond either to a progressive transitional climate after the warmer Noachian epoch (*7*) or to episodic warmer periods, such as those that could be related to the increase in atmospheric water vapor due to the outburst of outflow channels (*31*). Stable liquid water at the surface in the Hesperian epoch was previously suggested to explain potential lake deposits inside Candor Chasma (*18*) or in highland craters [e.g., (*32*)], and other Hesperian valley networks were noticed on highlands (*7*, *10*) and volcanoes (*7*, *9*). Such conditions could also solve the paradox of the ocean in the northern lowlands (*33*), which is dated to the Late Hesperian. Finally, longer term hydrological activity until the Late Hesperian would lead to interesting exobiological consequences, because life—if it ever existed on Mars—would have benefited from a longer period of warmer conditions.

References and Notes

1. R. P. Sharp, M. C. Malin, *Geol. Soc. Am. Bull.* **86**, 593 (1975).
2. D. C. Pieri, *Science* **210**, 895 (1980).
3. J. B. Pollack, J. F. Kasting, S. M. Richardson, K. Poliakoff, *Icarus* **71**, 203 (1987).

4. M. H. Carr, *Water on Mars* (Oxford Univ. Press, New York, 1996).
5. H. J. Masursky, *J. Geophys. Res.* **78**, 4009 (1973).
6. C. Sagan, O. B. Toon, P. J. Gierasch, *Science* **181**, 1045 (1973).
7. R. A. Craddock, A. D. Howard, *J. Geophys. Res.* **107** (E11), 10.1029/2001JE001505 (2002).
8. M. C. Malin, K. S. Edgett, *Science* **302**, 1931 (2003).
9. V. C. Gulick, V. R. Baker, *J. Geophys. Res.* **95**, 14325 (1990).
10. J. M. Dohm, K. L. Tanaka, *Planet. Space Sci.* **47**, 411 (1999).
11. J. E. Laity, M. C. Malin, *Geol. Soc. Am. Bull.* **96**, 203 (1985).
12. Sapping is a consequence of the infiltration of water from rainfall or snowmelt that induces groundwater flow and seepage, forming valleys with theater-shaped heads.
13. R. C. Kochel, J. F. Piper, *J. Geophys. Res.* **91** (suppl.), 175 (1986).
14. J. M. Goldspiel, S. W. Squyres, *Icarus* **148**, 176 (2000).
15. P. R. Christensen *et al.*, *Science* **300**, 2061 (2003); published online 5 June 2003 (10.1126/science.1080885).
16. The geology of Mars is divided into three main periods, Noachian, Hesperian, and Amazonian. The Noachian period (>3.6 billion years ago) (*17*) is a period of heavy bombardment and potential warmer climate. The Hesperian age (3.6 to 2.9 billion years ago) is usually considered to be cold with a thick permafrost (*4*).
17. W. K. Hartmann, G. Neukum, *Space Sci. Rev.* **96**, 165 (2001).
18. B. K. Lucchita *et al.*, in *Mars*, H. H. Kieffer, B. M. Jakosky, C. W. Snyder, M. S. Matthews, Eds. (Univ. of Arizona Press, Tucson, AZ, 1992), pp. 453–492.
19. C. M. Weitz, T. J. Parker, M. H. Bulmer, F. S. Anderson, J. A. Grant, *J. Geophys. Res.* **108** (E12), 10.1029/2002JE002022 (2003).
20. M. C. Malin, M. H. Carr, *Nature* **397**, 589 (1999).
21. A portion of channel was observed in Nanedi valles, northeast of the Valles Marineris region, and was interpreted as evidence for sustained liquid flow.
22. M. H. Carr, F. C. Chuang, *J. Geophys. Res.* **102**, 9145 (1997).
23. R. E. Horton, *Geol. Soc. Am. Bull.* **82**, 1355 (1945).
24. L. B. Leopold, M. G. Wolman, J. P. Miller, *Fluvial Processes in Geomorphology* (Dover, New York, 1992).
25. L. F. Phillips, S. A. Schumm, *Geology* **15**, 813 (1987).
26. G. D. Clow, *Icarus* **72**, 95 (1987).
27. M. H. Carr, J. W. Head, *Geophys. Res. Lett.* **30** (no. 24), 2245 (2003).
28. J. Menzies, W. W. Shilts, in *Past Glacial Environments*, J. Menzies, Ed. (Butterworth-Heinemann, Oxford, UK, 1996), pp. 15–136.
29. Inversion of relief occurs by denudation in cases where a material at the floor of a channel is more resistant to erosion than is the surrounding material. Similar inverted channels may exist on West Juventae Chasma plateau [reference 13 in (*8*)].
30. K. L. Tanaka, D. H. Scott, R. Greeley, in *Mars*, H. H. Kieffer, B. M. Jakosky, C. W. Snyder, M. S. Matthews, Eds. (Univ. of Arizona Press, Tucson, AZ, 1992), pp. 345–382.
31. V. R. Baker *et al.*, *Nature* **352**, 589 (1991).
32. N. A. Cabrol, E. A. Grin, *Icarus* **149**, 291 (2001).
33. T. J. Parker, D. S. Gorsline, R. S. Saunders, D. C. Pieri, D. M. Schneeberger, *J. Geophys. Res.* **98**, 11061 (1993).
34. We thank the THEMIS team for quick release of data (http://themis-data.asu.edu) and F. Forget and G. Dromart for helpful discussions. Supported by Programme National de Planétologie, Institut National des Sciences de l'Univers, France.

Supporting Online Material
www.sciencemag.org/cgi/content/full/305/5680/78/DC1
Figs. S1 to S3
Table S1
References

4 March 2004; accepted 24 May 2004

The Normal Function of a Speciation Gene, *Odysseus*, and Its Hybrid Sterility Effect

Sha Sun,[1]* Chau-Ti Ting,[2] Chung-I Wu[1]†

To understand how postmating isolation is connected to the normal process of species divergence and why hybrid male sterility is often the first sign of speciation, we analyzed the *Odysseus* (*OdsH*) gene of hybrid male sterility in *Drosophila*. We carried out expression analysis, transgenic study, and gene knockout. The combined evidence suggests that the sterility phenotype represents a novel manifestation of the gene function rather than the reduction or loss of the normal one. The gene knockout experiment identified the normal function of *OdsH* as a modest enhancement of sperm production in young males. The implication of a weak effect of *OdsH* on the normal phenotype but a strong influence on hybrid male sterility is discussed in light of Haldane's rule of postmating isolation.

The evolution of reproductive isolation is an intriguing process. Obviously, there is no advantage for a gene to induce inviability or sterility. Postmating isolation mechanisms such as hybrid sterility must be a by-product of species divergence or, more specifically, functional divergence of the underlying genes (*1*). Therefore, to understand the molecular mechanisms of speciation, we need to study the individual genes and ask the two following questions: (i) what are the normal functions of genes of reproductive isolation? and (ii) what is the connection between the normal function in the pure species and the incompatibility effect in the hybrids?

We address these questions by studying the hybrid male sterility gene, *OdsH* (*Odysseus*), in *Drosophila*. *OdsH* is a fast-evolving homeobox gene that causes male sterility in the *D. simulans* background when co-introgressed with closely linked factors from *D. mauritiana* (*2*, *3*). Divergence in *OdsH* among closely related species has been observed for both DNA sequences and expression patterns. *OdsH* has been evolving away from the ancestral embryonic function toward a predominantly spermatogenic expression (*4*). We used three approaches, gene expression assay, gene transformation, and gene knockout, to link the hybrid sterility effect of *OdsH* to its normal function in reproduction. The expression analysis was carried out with RNA in situ hybridization in the testes of fertile and sterile hybrids (Fig. 1). The fertile and sterile lines we used differ by only 3 kb, which spans the exons 3 and 4 of *OdsH* (fig. S1) (*2*), but are otherwise genetically identical. Figure 1A shows the expression of *OdsH* in the sterile introgression line. The striking observation is the strong accumulation of the *OdsH* transcript near the apical tip of the testis. This distinct pattern is not observed in the fertile line (Fig. 1B), nor in any of the pure species assayed, including *D. simulans* and *D. mauritiana* (*4*). The apical region of the testis contains primarily premeiotic cells that have not yet entered the rapid growth phase when transcription becomes highly active (*5*). Apparently, the testicular expression of *OdsH* is misregulated in the sterile introgression line. We reproduced this expression pattern for a comparison with the expression of *unc-4*, the duplicate homolog of *OdsH* (fig. S2). The expression of *unc-4* shows no transcript accumulation at the apical end and is comparable between the sterile (fig. S2C) and the fertile (fig. S2D) lines.

In addition to the misexpression of *OdsH*, we tested the sterility effect from *OdsH* coding sequence using transgenic analysis. *OdsH* full-length cDNA was driven by the testis-specific β*2-tubulin* promoter (*6*, *7*). We used *OdsH* alleles from *D. simulans* ($OdsH^{sim}$) and *D. mauritiana* ($OdsH^{mau}$). The P-element constructs, $P\{w^+, \beta 2\text{-}tubulin::OdsH^{sim}\}$ and $P\{w^+, \beta 2\text{-}tubulin::OdsH^{mau}\}$, were each injected into *D. simulans*, and the expression of each transgene was confirmed by reverse transcription polymerase chain reaction. We observed no sterility effect with the transgenes (heterozygous or homozygous) in the pure *D. simulans* background. This observa-

[1]Department of Ecology and Evolution, University of Chicago, Chicago, IL 60637, USA. [2]Department of Life Science, National Tsing Hua University, Hsinchu, Taiwan 300, ROC.

*Present address: Department of Molecular and Cell Biology, University of California, Berkeley, 16 Barker Hall, MC 3204, Berkeley, CA 94720, USA.
†To whom correspondence should be addressed. E-mail: ciwu@uchicago.edu